Nanobioceramic Composites: A Study of Mechanical, Morphological, and Thermal Properties

Sivabalan Sasthiryar,[a] H. P. S. Abdul Khalil,[a]* A. H. Bhat,[b] Z. A. Ahmad,[c] Md Nazrul Islam,[a,d], A. Zaidon,[e] and Rudi Dungani [a,f]

The aim of this study was to explore the incorporation of biomass carbon nanofillers (CNF) into advanced ceramic. Biomass from bamboo, bagasse (remains of sugarcane after pressing), and oil palm ash was used as the predecessor for producing carbon black nanofillers. Furnace pyrolysis was carried out at 1000 °C and was followed by ball-mill processing to obtain carbon nanofillers in the range of 50 nm to 100 nm. CNFs were added to alumina in varying weight fractions and the resulting mixture was subjected to vacuum sintering at 1400 °C to produce nanobioceramic composites. The ceramic composites were characterized for mechanical, thermal, and morphological properties. A high-resolution Charge-coupled device (CCD) camera was used to study the fracture impact and the failure mechanism. An increase in the loading percentage of CNFs in the alumna decreased the specific gravity, vickers hardness (HV), and fracture toughness values of the composite materials. Furthermore, the thermal conductivity and the thermal stability of the ceramic composite increased as compared to the pristine alumina.

Keywords: Ceramic composite; Carbon nanofiller; Thermogravimetric Analysis; Mechanical properties

*Contact information: a: School of Industrial Technology, Universiti Sains Malaysia, 11800, Penang, Malaysia; b: Department of Fundamental and Applied Sciences, Universiti Teknologi Petronas, 31750 Tronoh, Perak, Malaysia; c: School of Mineral and Material Engineering, Universiti Sains Malaysia, 14000 Transkrian, Penang, Malaysia,; d: School of Life Science, Khulna University, Khulna 9208, Bangladesh; e: Universiti Putra Malaysia, Faculty of Forestry, Serdang, 43400 Selangor, Malaysia; ,f: School of Life Sciences and Technology, Institut Teknologi Bandung, Gedung Labtex XI, Jalan Ganesha 10, Bandung 40132, West Java-Indonesia; *Corresponding author: akhalilhps@gmail.com*

INTRODUCTION

Biomass as a precursor of carbon is well known as an active material for energy storage and conversion. Natural lignocellulosic fiber has a high carbon content and good properties. Jute, flax, coconut shells, oil palm, bamboo, bagasse, and oil palm ash are natural fibers that contain high carbon content (Abdul Khalil *et al.* 2009). The preferred source of carbon nanofiller (CNF) in this study is biomass, which is abundantly available as waste from the agricultural activities in Malaysia. Specifically, biomass from bamboo (*Gigantochloa scoretechinii*), bagasse, and oil palm ash is generally used as a precursor of carbon black. CNF is extremely porous, has a large surface area, and is typically produced from organic precursors such as bamboo, bagasse, coconut shells, palm-kernel shells, wood chips, sawdust, corncobs, and seeds.

Carbon materials have a naturally high electrical conductivity and low cost, high surface area, porosity, and formability, and possess good chemical and electrochemical resistivity (Mudimela *et al.* 2009). Carbon black is a form of amorphous carbon that has an extremely high surface area to volume ratio. As such, it is one of the first nano-

materials to be commonly used (Mudimela *et al*. 2009). With the novel discovery of carbon nanotubes (CNTs) and nanofillers (CNFs) material, having unique geometrical structure, stable mechanical and chemical properties, it has attracted wide scale attention in many sectors (Mudimela *et al*. 2009). Predominantly, carbon black is used as a pigment and for reinforcement in rubber and plastic products. The use of carbon nanofillers in various industries is related to properties of specific surface area, particle size, structure, conductivity, and color (Saito *et al*. 1998). Besides, the use of carbon nanofillers in polymer can increase the hardness depending on the carbon structure. Therefore, small additions of CNTs and CNFs to different materials can considerably improve their mechanical and electrical properties (Riggs *et al*. 2000; Jong and Geus 2000; Wagner *et al*. 1998). CNT/CNF reinforced cement composites are able to provide electromagnetic interference shielding (Fu and Chung 1996) and are also capable of non-destructive flaw detection (Chen and Chung 1993). Utilization of CNTs/CNFs has already been occasionally investigated for applications in the electronic and construction industries, although the expected improvement has not been fully achieved (Li *et al*. 2005; Chung 2001).

Nevertheless, the addition of CNF greatly enhances the electrical properties of insulating ceramics, allowing electrical discharge machining to be used to manufacture intricate parts. Meanwhile, other properties of the ceramic may be either preserved or even improved. With this, new opportunities for the manufacture of complicated ceramic parts by adding CNF can be achieved for new engineering and biomedical applications. Since the discovery of CNFs, there has been a great deal of attention due to their exceptional properties (Calvert 1993; Zhu *et al*. 2004; Makar and Beaudoin 2004), including their use as nanofillers in ceramic materials in order to develop tougher composites (Wenig *et al*. 1997). While the contribution of CNFs as a reinforcement phase in ceramics is still under debate (Hernadi *et al*. 1996), other characteristics have been considerably enhanced such as the tribological (Qingwen *et al*. 2002; An and Lim 2002) and the electrical properties (Sener *et al*. 2004; Sevcik and Skvara 2001). Recent work in the increase of the grindability of Si_3N_4/CNT composites compared to the monolithic material has also been demonstrated (Nasibulin *et al*. 2006). However, the material properties of CNF ceramic composites have not been reported before.

This study has been carried out to investigate the effects of varying the loading percentage of CNF in an alumina matrix on the properties of the composite. The morphological study was further conducted to understand the interaction between the CNF and alumina matrix.

EXPERIMENTAL

Materials

A desirable amount of carbon nanomaterial was introduced into the matrix to produce the ceramic composites. CNF particles with sizes from 50 to 100 nm were chosen as a model object for the comparative study of CNFs in ceramics. CNFs were produced at a temperature of 1000 °C by furnace pyrolysis. This was followed by ball-mill processing of carbon black from bamboo, bagasse, and oil palm ash. In addition, alumina was used as a baseline material because of its superior chemical and thermo-mechanical characteristics in engineering applications. A monolithic Al_2O_3 having an average particle size of 0.5 μm and 99% purity (Martinswerck) was selected. The ceramic

composite samples were prepared at different wt.% of CNF with Al_2O_3 as the baseline material. The CNF loading percentages were 0.00, 0.05, 0.1, 0.5, and 1.0% except for specific gravity where the incremental load percentages were 0 to 20%. This was done to find out the impact of CNF loading on specific gravity of ceramic matrix. CNF and Al_2O_3 in powder form were then mixed evenly and were pressed at 295 MPa using a hydraulic press. The ceramic composite was then sintered in a Lenton electric hearth vacuum furnace at 1400 °C for 4 h at a 5 °C/min sintering rate.

Methods

Mechanical properties

Sintered ceramic composite samples were subjected to Vickers hardness (HV20) testing for measuring the hardness of the matrix in which hardness number is determined by the load over the surface area of the indentation and not the area normal to the force. The size of the samples was 11.56 mm (diameter) x 3.4 mm (thickness). Fracture toughness was calculated from the Vickers hardness data according to Eq. 1, as proposed by Niihara *et al.* (1982). All tests were carried out at room temperature. An Electronic Densitometer (MD-2005) was used to measure the density based on the density of water at 4 °C (1g/cm^3).

$$3K_{1c} = 0.035(Ha^{1/2})(3E/H)^{0.4}(l/a)^{-0.5} \quad (1)$$

In Eq. 1, K_{1c} is the fracture toughness, H is Vickers hardness, a is the half length of Vickers diagonal (μm), E is the Young modulus of the samples, and l is the length of the radial crack size (μm).

Thermal properties

A Perkin Elmer thermal gravimetric analyser (TGA-6) was used to investigate the stability of the ceramic composite. The ceramic composites (4 to 5 mg) were heated from 30 °C to 1000 °C at a heating rate of 20 °C/min under a nitrogen environment. A Hot Disk Thermal Constants Analyser (TPS2500S) at 0.06 Watt per 30 seconds was used to study the thermal conductivity and to measure the Specific Heat.

Morphological properties

A morphological study of the impact of the fractured ceramic composite was carried out by using an SEM with a high-resolution CCD camera (Model: JAI CV-A1, resolution1296×1024 pixels) fitted with a 50 mm lens and a 110 mm extension tube on the cracked surface. Backlighting was used to highlight the profile of the tool. The field-of-view of the CCD camera was 2.3×2.0 mm, and the distance from the front end of camera lens to the cutting tool was approximately 60 mm. The micro-structure analysis was done by using transmission electron microscope (TEM) at the cross-sections of the samples.

RESULTS AND DISCUSSION

Mechanical Properties

The effect of CNF loading on the Vickers hardness (HV20) is shown in Fig. 1. With respect to the pristine alumina, the hardness strength showed a similar trend for

each series of CNFs. A decreasing trend was observed for all samples. Teng *et al*. (2007) stated that additives with smaller particles were easily densified and were more active due to high surface activity during the sintering process compared to additives with larger particle sizes.

The decrease in Vickers hardness was attributed to the small grain size of CNF nanostructures, which could result in the microstructure pinning effect in alumina. The decrease in the hardness of alumina-CNF ceramic composites was mainly due to grain growth inhibition, which increased the density of the ceramics during vacuum sintering. The higher density increased the hardness of ceramic matrix to a certain level; however, the density decreased after that.

Similar results were also reported by Vasylkiv *et al*. (2003). This is also observed in case of the specific gravity (SG) analysis, which shows that the SG decreases as the CNF wt.% increases. Figure 2 shows the effect of CNF percent loading on the specific gravity of ceramic composites.

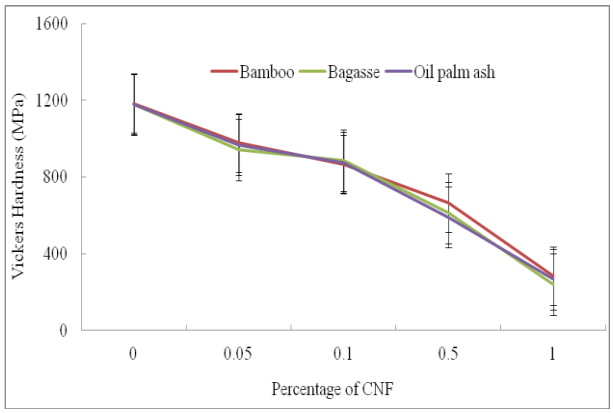

Fig. 1. Effects of CNF percentage on hardness strength of ceramic composites

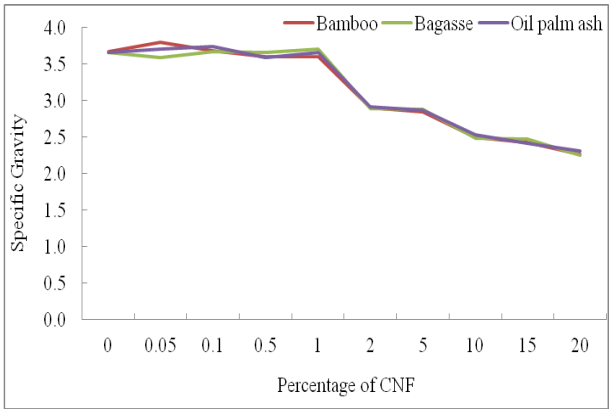

Fig. 2. Effects of CNF percentage on specific gravity of ceramic composites

Similar work by Amin *et. al.* (2009) shows that the bulk density of the composites is reduced with increasing nano carbon black content in the samples. This is due to lower density of the nano carbon black compared with the density of the other components.

Densities of the sintered ceramic composite were determined using the Archimedes principle. Alumina-CNF ceramic composite shows a slight variable increase in density as the loading increases to 1% compared to the pure alumina. A significant decrease was observed when the loading increased from 2% to 20%, which makes the ceramic composite much lighter than alumina. Figure 3 indicates the results of the fracture toughness tests of alumina-CNF.

The decrease in fracture toughness is mainly due to cracked bridging of the nano grains of CNFs formed onto alumina particles. This makes the ceramic composite brittle as the loading percentage increases. The previous study by Riu *et al*. (2000) concluded that the increase of fracture toughness is mainly due to the large elongated or platelike grain formation in the microstructure. On the contrary, the decrease observed in alumina-CNF is largely due to the level of undoped specimen contained in the pores of the ceramic composite sample. With this understanding, it is acknowledged that the alumina-CNF ceramic composite becomes lighter and more brittle as the CNF loading increases.

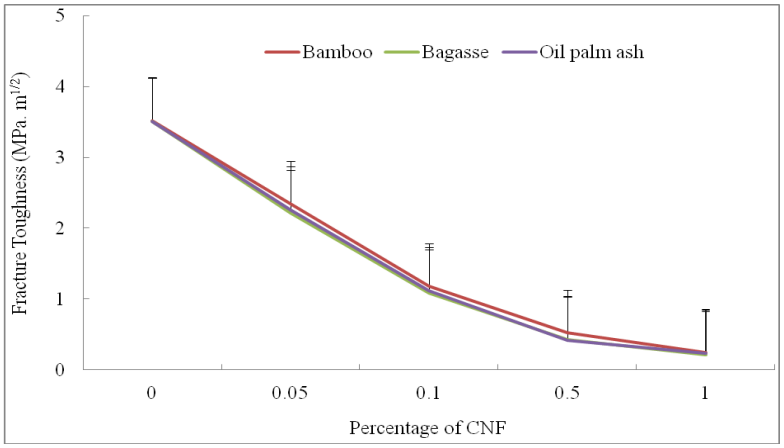

Fig. 3. Effects of CNF percentage on fracture toughness of ceramic composites

Morphological Properties

The microstructure of the alumina-CNF composite can be observed in Fig. 4. The figure also shows the development of cracks and its progress in the ceramic matrix. The white spots in the figures show the distribution of CNFs in the matrix. As the loading percent increases, the amount of cracks and the crack elongation increases and the sample becomes brittle.

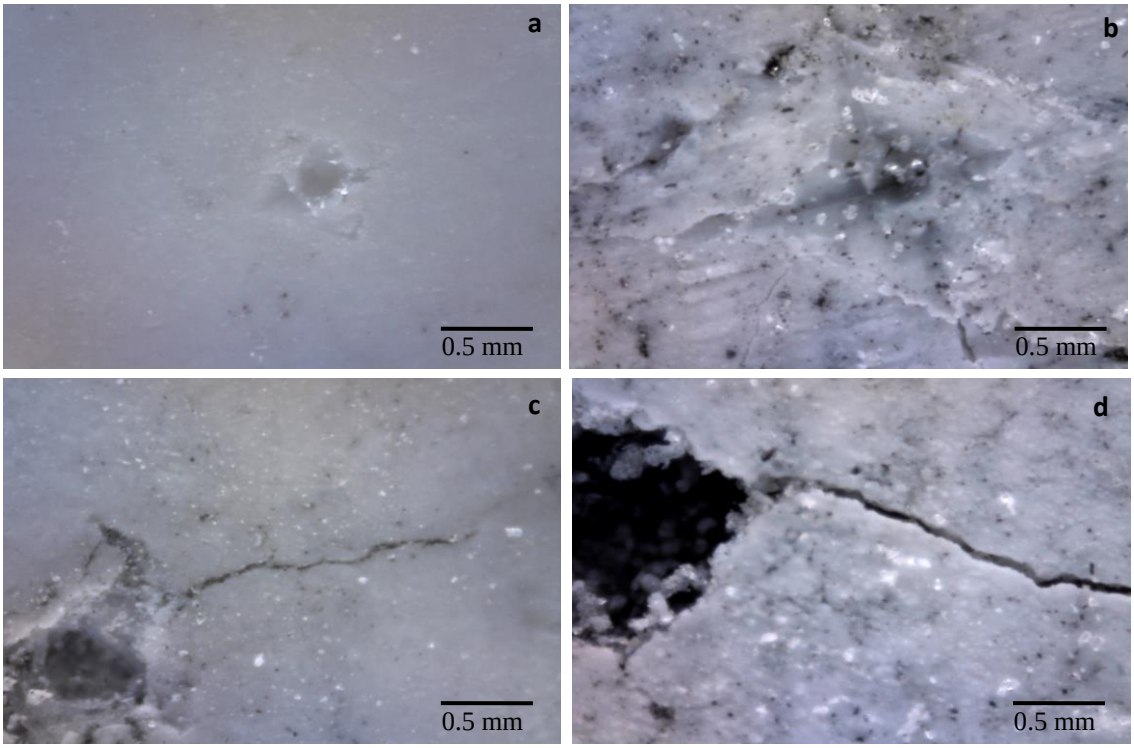

Fig. 4. SEM micrograph of Alumina-CNF ceramic composite at (a) 0%, (b) 0.05%, (c) 0.1%, and (d) 0.5% CNF loading

A previous study showed that cracks fail to propagate because of grain mismatch and the consequent poor bonding between the nano-carbon black and the ceramic phase (Riggs *et al*. 2000).

Transmission electron microscopy (TEM) was used to study the size and nanocrystalline orientation of the carbon nanofibers (Fig. 5). The figure also shows that the CNF particles were not evenly distributed in the ceramic matrix. This uneven distribution of CNF particles into the matrix affected the fracture toughness. TEM technique provides information on a very local scale about the particle size. TEM is a valuable tool because it enables us to see the filler on a nanometer scale. The micrograph provides information regarding the likely sizes of particles present in the sample. The particle sizes on the TEM image are worth noting and ranged from 20 to 40 nm. Nanoparticles showed agglomeration in some parts due to their conformation.

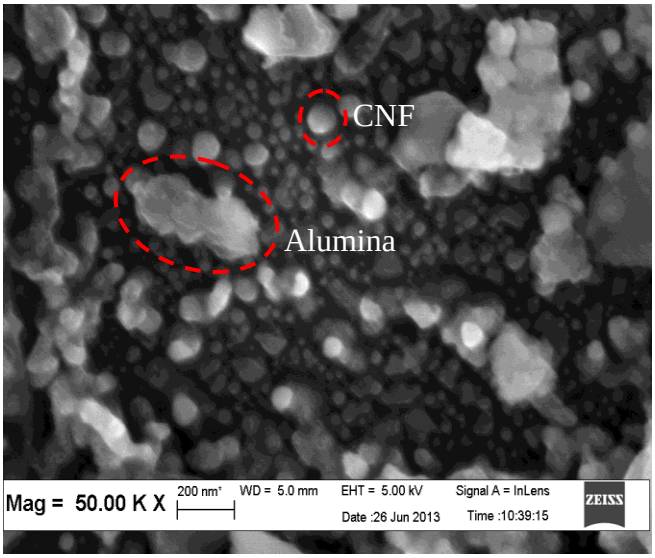

Fig. 5. TEM micrograph of carbon nanofiber

Thermal Properties

TGA thermograms (Fig. 6) show the decomposition of the alumina-CNF ceramic composite at higher temperatures compared to CNF alone.

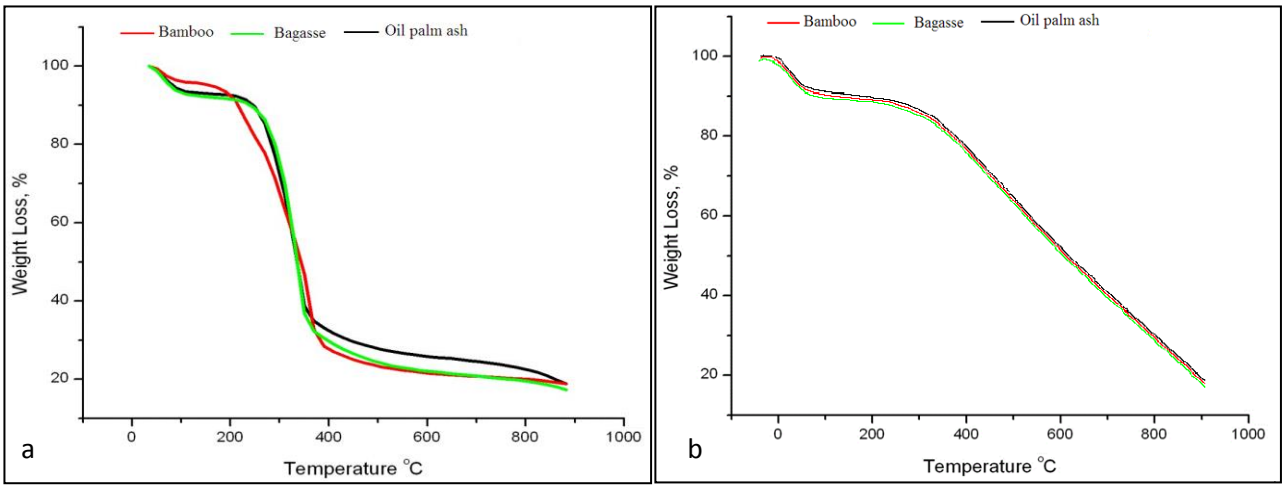

Fig. 6. Thermal degradation of (a) CNFs and (b) Alumina-CNF ceramic composite

Figure 6a shows thermograms of different CNFs, while Fig. 6b provides thermograms of alumina-CNF based ceramic composites. The CNFs exhibited two stages of degradation, whereas the ceramic composite showed only a single stage. Jawaid *et al.* (2013) studied the thermal properties of oil palm epoxy composite, which also showed a two stage thermal degradation. Initially, all CNFs undergo a dehydration process in which about 5±2% of water is removed by vapourisation at 100 °C. The critical mass reduction occurs at 250 to 375 °C, where the weight loss is >50%. The high temperature weight loss is relatively small due to the left over amount of residue. According to Munir *et al*. (2009), the weight loss associated with moisture evaporation and thermal degradation of all raw materials will give an initial weight loss below 100 °C. All series of ceramic composite seemed to be stable, and less decomposition took place at even higher temperatures (Fig. 6b). The glass-transition temperature (T_g) is the most important property in determining the suitability of a polymer for an engineering application. Despite its importance, determining the underlying mechanisms that govern the T_g phenomenon remains one of the outstanding challenges in polymer physics (Munir *et al.* 2009). A study by Ash *et al.* (2004) concluded that the thermal behaviour of polymer composites depends strongly on the matrix polymer and its chemical and morphological characteristics. In the study, similar behaviour was observed for alumina-CNF ceramic composite where T_g behaviour corresponded strongly with alumina characteristics. The addition of the CNF had little effect on the alumina matrix. Alumina-CNF's thermal transformation depends on the crystalline phase of the CNF porosity structure. Since at temperatures between 200 to 400 °C, carbon reacts with oxygen and becomes transformed to the vapours of CO_2, alumina alone is left in the amorphous phase.

The property that characterizes the ability of a material to transfer heat is the thermal conductivity. In steady-state heat transport, the flux is proportional to the temperature gradient along the direction of flow where the proportionality is constant (Maleka *et al.* 2006). Thermal conductivity is shown in Fig. 7 and indicates that as the loading (wt.%) of CNF in the alumina matrix increased, the thermal conductivity equally showed an increase. Alumina, a nonmetallic material is a thermal insulator because of its lack of a large amount of free electrons (Maleka *et al*. 2006). Thus, the phonons (lattice vibration waves) are primarily responsible for thermal conduction in ceramics which are comparatively weaker than the free electrons transportation process. The phonons are not as effective as free electrons in the transport of heat energy due to efficient phonon scattering by lattice imperfections.

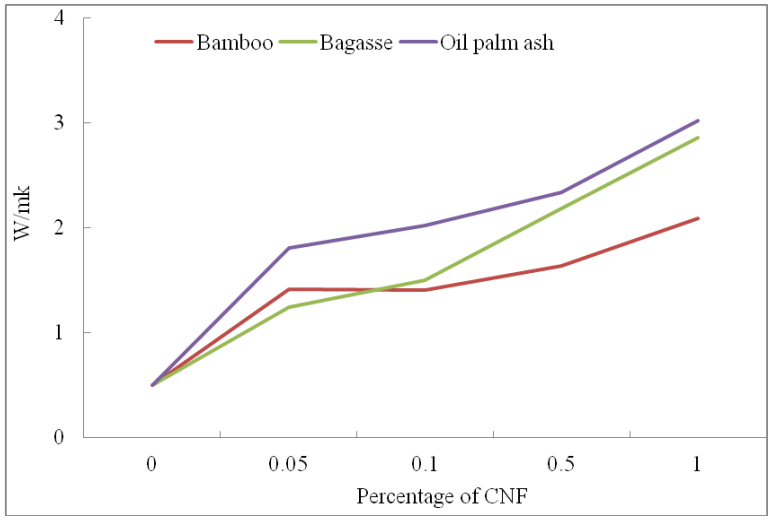

Fig. 7. Effects of CNF percent loading on the thermal conductivity of Alumina-ceramic composites

With the addition of CNF into the alumina matrix, the new ceramic composite possesses free electrons, giving rise to thermal conductivity. Within the CNFs, oil palm ash ceramic composite gives a large thermal conductivity and bamboo-based composite gives a lower thermal conductivity. This is mainly due to the higher inorganic composition of oil palm compared to bamboo, which gives more lattice ionic influence on thermal conductivity.

The scattering of lattice vibrations becomes more pronounced with rising temperature; hence, the thermal conductivity of most ceramic materials normally diminishes with increasing temperature, prominent at relatively low temperature (Maleka *et al*. 2006). Heat transfer across pores is ordinarily slow and inefficient. Internal pores normally contain still air, which has an extremely low thermal conductivity of approximately 0.02 W/m-K (Maleka *et al*. 2006). Figure 7 indicates that the conductivity begins to increase at higher loading. This is due to radiant heat transfer.

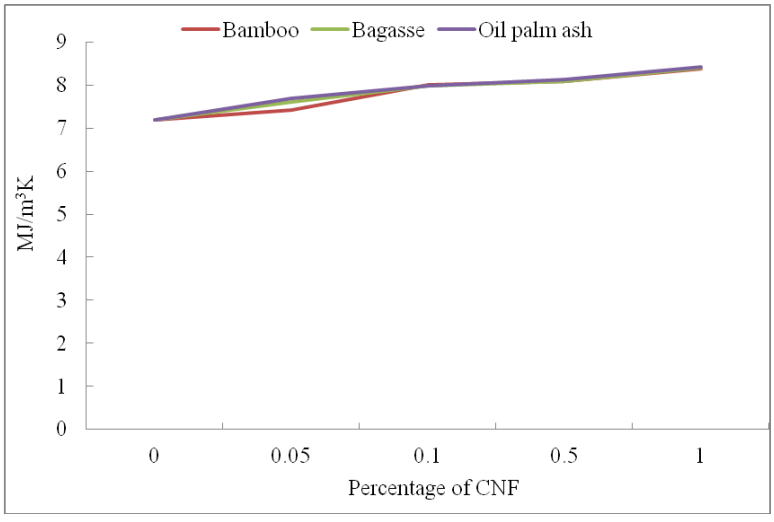

Fig. 8. Effects of CNF loading percentage on the specific heat of Alumina-ceramic composites

In the case of specific heat, Fig. 8 shows that a significant quantity of radiant heat may be transported through a transparent alumina-CNF ceramic composite. Specific heat often represents the heat capacity per unit mass (Maleka *et al*. 2006). Porosity in alumina ceramic materials might have a dramatic influence on the thermal conductivity. Thus, the thermal conductivity increases with the increase of CNFs' pore volume. Figure 8 shows the increase in specific heat as the CNFs' loading increases. All types of CNFs showed a similar response of increase in specific heat when the loading increased. Amin *et al.* (2009) also showed that the relative heat resistance of composites increased with the loading percentage of CNF because the pores and voids were filled by CNF particles rather than gels. Because of this, the structure of the castable composites is not compacted and stresses can be relaxed under the influence of heating cycles.

CONCLUSIONS

1. The Vickers hardness and fracture toughness decreased gradually with the increase of CNF percent loading. Specific gravity also declined with the increase of CNF percent loading. Thus, the new alumina-CNF ceramic composite is lighter but more brittle compared to the pristine alumina.
2. Thermal conductivity and specific heat increased in alumina-CNF ceramic composite compared to the others. Thus, incorporation of CNF into alumina matrix gives lighter, stable, and more thermally conductive composites which can be used in advanced packaging.

ACKNOWLEDGEMENTS

The researchers would like to thank the Universiti Sains Malaysia, Penang for providing research Grant RU-I 1001/PTEKIND/814133 and RU-1001/PTEKIND/811195 that have made this work possible.

REFERENCES CITED

Abdul Khalil, H. P. S., Kang, C. W., Khairul. A., Ridzuan. R., and Adawi, T. O. (2009). "The effect of different laminations on mechanical and physical properties of hybrid composite," *J. Reinf. Plast. Compos.* 28(9), 1123-1137.

Amin, M. H., Mohsen, A. E., and Mohamad, R. R. (2009). "The effect of nanosized carbon black on the physical and thermomechanical properties of Al_2O_3–SiC–SiO_2–C composite," *J. Nanomaterials* 325674, 1-5.

An, J. W., and Lim, D. S. (2002). "Synthesis and characterization of alumina/carbon nanotube composite powders," *J. Ceram. Process. Res.* 3, 174-177.

Ash, B. J., Siegel, R. W., and Schadler, L. S. (2004). "Glass-transition temperature behavior of alumina/PMMA nanocomposites," *J. Polym. Sci. Pol. Phys.* 42(23), 4371-4383.

Calvert, P. (1993). "Nanotube composites: A recipe for strength," *Nature* 399, 210-211.

Chen, P. W., and Chung, D. D. L. (1993). "Carbon fiber reinforced concrete for smart structures capable of non-destructive flaw detection," *Smart Mater. Stru.* 2(1), 22-30.

Chung, D. D. L. (2001). "Comparison of submicron-diameter carbon filaments and conventional carbon fibers as fillers in composite materials," *Carbon* 39(8), 119-1125.

Fu, X., and Chung, D. D. L. (1996). "Submicron carbon filament cement-matrix composites for electromagnetic interference shielding," *Cement Concrete Res.* 26(10), 1467-1472.

Hernadi, K., Fonseca, A., Nagy, J. B., Bernaerts, D., Riga, J., and Lucas, A. (1996). "Catalytic synthesis and purification of carbon nanotubes," *Synthetic Met.* 77(1-3), 31-34.

Jawaid, M., Abdul Khalil, H. P. S., Bakar, A. A., Hassan, A., and Dungani, R. (2013). "Effect of jute fibre loading the mechanical and thermal properties of oil palm-epoxy composite," *J. Compos. Mater.* 47, 1633-1641.

Jong, K. P. D., and Geus, J. W. (2000). "Carbon nanofibers: Catalytic synthesis and applications catalysis reviews," *Sci. Eng.* 42(4), 481-510.

Li, G. Y., Wang, P. M., and Zhao, X. (2005). "Mechanical behavior and microstructure of cement composites incorporating surface-treated multi-walled carbon nanotubes," *Carbon* 43(6), 1239-1245.

Makar, J. M., and Beaudoin, J. J. (2004). "Carbon nanotubes and their application in the construction industry," *Proceedings of 1st International Symposium on Nanotechnology in Construction* 2004, Paisley, Scotland, pp. 331-334.

Maleka, O., González-Juliánc, J., Vleugelsb, J., Vanderauwera, W., Lauwers, B., and Belmonte, M. (2006). "Carbon nanofillers for machining insulating ceramics," *MaterialToday* 14(10), 496-501.

Mudimela, P. R., Nasibulina, L. I., Nasibulin, A. G., Cwirzen, A., Valkeapää, M., Habermehl-Cwirzen, K., Malm, J. E. M., Karppinen, M. J., Penttala, V., Koltsova, T. S., Tolochko, O. V., and Kauppinen, E. I. (2009). "Synthesis of carbon nanotubes and nanofibers on silica and cement matrix materials," *J. Nanomaterials* 2, 1-4.

Munir, S., Daood, S., Nimmo, W, Cunliffe, A. M., and Gibbs, B. M. (2009). "Thermal analysis and devolatilization kinetics of cotton stalk, sugar cane bagasse and shea meal under nitrogen and air atmospheres," *Bioresource Technol.* 100(3), 1413-1418.

Nasibulin, A. G., Brown, D. P., Queipo, P., Gonzalez, D., Jiang, H., and Kauppinen, E. (2006). "An essential role of CO_2 and H_2O during single-walled CNT synthesis from carbon monoxide," *Chem. Phys. Lett.* 417(1-3), 179-184.

Niihara K., Morena R. and Hasselman D. P. H. (1982). "Evaluation of K_{IC} of brittle solids by the indentation method with low crack-to-indentation ratios," *J. Mater. Sci. Lett.* 1(1), 13-16.

Qingwen, L., Hao, Y., Yan, C., Jin, Z., and Zhongfan, L. (2002). "A scalable CVD synthesis of high-purity single-walled carbon nanotubes with porous MgO as support material," *J. Mater. Chem.* 12, 1179-1183.

Riggs, J. E., Guo, Z. X., Carroll, D. L., and Sun, Y. P. (2000). "Strong luminescence of solubilized carbon nanotubes," *J. Am. Chem. Soc.* 122(24), 5879-5888.

Riu, D. H., Kong, Y. M., and Kim, H. E. (2000). "Effect of Cr_2O_3 addition on micro-structural evolution and mechanical properties of Al_2O_3," *J. Eur. Ceram. Soc.* 20(10), 1475-1481.

Saito, R., Dresselhaus, G., and Dresselhaus, M. S. (1998). *Physical Properties of Carbon Nanotubes*, Imperial College Press: London.

Sener, S., Bilgen, S., and Özbayoglu, G. (2004). "Effect of heat treatment on grindabilities of celestite and gypsum and separation of heated mixture by differential grinding," *Miner. Eng.* 17(3), 473-475.

Sevcik, V., and Skvara, F. (2001). "High temperature-properties of a binder on gypsum-free portland cement over the temperature 20 to 1200 °C," *Ceramics – Silikáty* 45(4), 151-157.

Teng, X., Liu, H., and Huang, C. (2007). "Effect of Al_2O_3 particle size on the mechanical properties of alumina-based ceramics," *Mater. Sci. Eng.* 452-453, 545-551.

Vasylkiv, O., Sakka, Y., and Skorokhod, V. V. (2003). "Hardness and fracture toughness of alumina-doped tetragonal zirconia with different yttria contents," *Mater. Trans.* 44(10), 2235-2238.

Wagner, H. D., Lourie, O., Feldman, Y., and Tenne, R. (1998). "Stress-induced fragmentation of multiwall carbon nanotubes in a polymer matrix," *Appl. Phys. Lett.* 72(2), 188-190.

Wenig, J. K., Langan, B. W., and Ward, M. A. (1997). "Pozzolanic reaction in Portland cement, silica fume, and fly ash mixtures," *Can. J. Civil Eng.* 24(5), 754-760.

Zhu, W., Bartos, P. J. M., and Porro, A. (2004). "Application of nanotechnology in construction," *Mater. Struct.* 37(9), 649-658.

Article submitted: October 3, 2013; Peer review completed: December 4, 2013; Revised version received and accepted: December 10, 2013; Published: December 18, 2013.